Scientific Research Publishing

Open Journal of Orthopedics, 2026, 16(3), 133-159
https://www.scirp.org/journal/ojo
ISSN Online: 2164-3016
ISSN Print: 2164-3008

Correlation of Disease Severity to Patient Synovial Fluid Characteristics and Development of a Simulated Synovial Fluid in Knee Osteoarthritis

Annie C. Bowles-Welch[1,2], Hazel Y. Stevens[1,2], Rebecca S. Schneider[2], Linda E. Kippner[1,2], Angela C. Jimenez[1,2,3], Theresa Kotanchek[4], Thanh N. Doan[5], David A. Frey Rubio[1,2], Carolyn Yeago[1,2], Hicham Drissi[5], Andrés J. García[2,6], Krishnendu Roy[7,8,9,10*]

[1]Marcus Center for Therapeutic Cell Characterization and Manufacturing, Georgia Institute of Technology, Atlanta, GA, USA
[2]Petit Institute for Bioengineering and Bioscience, Georgia Institute of Technology, Atlanta, GA, USA
[3]Department of Biomedical Engineering, Georgia Institute of Technology, Atlanta, GA, USA
[4]Evolved Analytics, LLC, Rancho Santa Fe, CA, USA
[5]Department of Orthopaedics, Emory University School of Medicine, Atlanta, GA, USA
[6]Woodruff School of Mechanical Engineering, Georgia Institute of Technology, Atlanta, GA, USA
[7]NSF Engineering Research Center (ERC) for Cell Manufacturing Technologies (CMaT), Atlanta, GA, USA
[8]Department of Biomedical Engineering, School of Engineering, Vanderbilt University, Nashville, TN, USA
[9]Department of Pathology, Microbiology, and Immunology, Vanderbilt University School of Medicine, Nashville, TN, USA
[10]Department of Chemical and Biomolecular Engineering, School of Engineering, Vanderbilt University, Nashville, TN, USA
Email: *krish.roy@vanderbilt.edu

How to cite this paper: Bowles-Welch, A.C., Stevens, H.Y., Schneider, R.S., Kippner, L.E., Jimenez, A.C., Kotanchek, T., Doan, T.N., Rubio, D.A.F., Yeago, C., Drissi, H., García, A.J. and Roy, K. (2026) Correlation of Disease Severity to Patient Synovial Fluid Characteristics and Development of a Simulated Synovial Fluid in Knee Osteoarthritis. *Open Journal of Orthopedics*, **16**, 133-159.
https://doi.org/10.4236/ojo.2026.163015

Received: March 16, 2026
Accepted: March 28, 2026
Published: March 31, 2026

Abstract

Knee osteoarthritis (OA) is a common degenerative disease resulting from pathological changes to the joint. Structural changes are radiographically identified to assess the severity of knee OA by the Kellgren-Lawrence (KL) scoring system; however, various risk and lifestyle factors contribute to the disease pathology and progression which complicate the assessment of OA severity and effective treatments. Growing evidence suggests that disease severity is closely tied to changes to the synovial fluid (SF) composition in OA-afflicted knees, which can modulate local cells. Thus, SF contains critical information about knee OA that can offer insight into the disease milieu. Herein, we characterized human OA patient-derived SF (pdSF) by measuring its molecular, physiological, and mechanical properties. Machine learning (ML) was used to correlate these data with either the corresponding KL scores or a grade of hyaluronic acid degradation based on a novel method as measures of OA. Results from ML models identified top variables in the pdSF as critical attributes, or potential predictors, of OA severity. Moreover, pdSF characterization in-

formed the development of an OA-simulated SF (simSF) which can be used as a surrogate when access to pdSF is limited. Using the simSF to mimic an OA environment, we developed *in vitro* assays to create: 1) a research tool to evaluate cell therapies (e.g., mesenchymal stromal cells (MSCs)), given their exposure to SF when injected intra-articularly, and 2) a pharmacological screening tool by incorporating local immune cells of the knee (e.g., macrophages). As a research tool, this OA-targeted potency assay can be used to elucidate donor-specific secretory responses by the MSCs, and quantifiable outcomes demonstrated that simSF elicited similar cellular responses compared to pdSF. We also demonstrated macrophage-specific secretory responses to simSF compared to pdSF that recapitulate OA-induced changes to these innate immune cells of the knee. This approach provides a tool for screening drug candidates directed toward macrophage-based mechanisms. Together, this study uncovered in-depth characteristics of pdSF, identified critical attributes of knee OA in pdSF that were correlative to OA severity, and developed a simSF product for *in vitro* testing that offers new opportunities for exploring knee OA disease and therapeutics.

Keywords

Osteoarthritis, Synovial Fluid, Potency Assays, Machine Learning

1. Introduction

Synovial fluid (SF) is a viscous liquid that provides lubrication, reducing friction between the articular cartilage surfaces during the movement of synovial joints [1]. SF also has metabolic and regulatory functions that are important for joint homeostasis [2]. SF is composed of various molecules that are derived from plasma and cells residing in multiple tissues of the joint, e.g. chondrocytes, synoviocytes, macrophages [3]. Osteoarthritis (OA) is a degenerative joint disease that affects the physiology of the joint compartment, thus mediating cellular and molecular changes including the composition of SF [3] [4]. Although change to the joint identified by radiography is used to diagnose OA severity according to the Kellgren-Lawrence (KL) score, no correlations between pain, functional scores, or patient factors to radiological severity of knee OA have yet to be identified [5]. Moreover, the severity of knee OA has not been correlated to molecular feature combinations in the synovial fluid from OA knees which could potentially provide objective measures to inform clinical decisions. Individual features that have been suggested include CCL13, Activin A, bone morphogenic protein-2, and CXCL12 [6]-[9]. As the pathogenesis of OA is not well understood and can differ greatly among individuals based on various risk factors and lifestyles, information about the interactions between the SF and local cells in an OA joint is limited. A better understanding of these molecular interactions by the presence of correlative features would provide valuable insights into OA pathogenesis, severity, and treatment.

Various proteins found in SF have been linked to the specific tissue in the knee

compartment where they originated [10], and studies have identified molecules such as cytokines, chemokines, and enzymes either as contributors to or are present as a result of OA pathogenesis. These molecules have been suggested as potential biomarkers of OA [3] [11] [12]. Protein components, the most abundant component of the SF, range in concentrations of 12 - 30 mg/mL in non-OA [13] subjects, but this can shift higher in OA patients (25 - 30 mg/mL) [14], a change presumably caused by altered permeability of the synovial membrane. Non-OA SF contains approximately 2.5 - 4.0 mg/mL hyaluronic acid (HA), a prevalent glycosaminoglycan that contributes to its viscosity. As SF volume increases within an OA joint, the HA concentration decreases, along with an increased presence of low molecular weight (MW) HA (<500 kDa) from degradation [15]. A shift in hyaluronan MW distribution curves to lower than 1 Da can indicate an increased incidence of joint space narrowing [16]. Together, reduced HA concentration, increased amounts of low MW HA, and decreased viscoelastic properties of SF are associated with increased pain in OA-afflicted knees [16].

OA is associated with chronic low-grade local and systemic inflammation, where fragmentation of the cartilage from damage activates synovial cells to release degradative enzymes and pro-inflammatory cytokines and chemokines. As cartilage proteoglycans break down in OA, keratan sulfate (KS) and chondroitin sulfate (CS) become present in SF [17]-[19]. Several of the components released when cartilage degenerates are known as damage-associated molecular pattern molecules which, under prolonged cellular stress, can promote Toll-like receptor signaling by pro-inflammatory mediators from macrophages and fibroblasts in the synovium [20]. Activated monocytes and macrophages produce inflammatory mediators, such as tumor necrosis factor-alpha (TNFα), interleukins (IL)-6, -8, -1β, and MMP-1,-3,-9 and -13 which have been detected in OA SF [21]-[23]. Furthermore, populations of senescent chondrocytes and macrophages in the synovium and peripheral blood release senescence-associated secretory phenotype-related proteins that activate the immune system [24]. This complex inflammatory signaling makes it difficult to precisely assess knee OA severity and is not represented by the KL scoring system.

The development and prescription of effective therapies to treat or slow the progression of OA are contingent on a better understanding of the knee OA severity. The KL score is based on radiological assessments of features related to knee damage in which a composite score from KL 0 (no OA) to KL 4 (severe OA) indicating OA severity. KL scores are visually determined by clinicians and do not describe changes to distinct knee compartments or histological features [25]. Oftentimes, it is these discrete features that can contribute to knee pain which have been investigated in nonclinical studies [26] [27]. Whereas the KL scoring system remains the gold standard for diagnosing knee OA, translation of SF characteristics could provide better indications of OA severity and improve treatment strategies.

For this study, OA patient-derived SF (pdSF; n = 41) samples were provided by the Multicenter Trial of Stem Cell Therapy for Osteoarthritis (MILES; NCT03818737)

clinical trial for comprehensive characterization analysis. pdSF samples were harvested from patients diagnosed as KL 2 (mild OA), KL 3 (moderate OA) or KL 4 (severe OA) and characterized for molecular composition, degree of HA degradation, and rheological properties. Machine learning analysis using symbolic regression models was then used to identify features of OA SF that were correlated to OA severity defined by KL score. This data also informed the development of an OA-simulated SF (simSF) product that can be used as a surrogate for pdSF when access to pdSF is limited. We developed *in vitro* assays that incorporated pdSF or simSF to mimic the OA microenvironment and demonstrated the use of these assays as valuable research and pharmacological screening tools. This study demonstrated an in-depth analysis of molecular and viscoelastic properties of pdSF to better correlate features of OA SF to OA severity compared to the standard KL score. The development and utility of simSF for *in vitro* assays demonstrated a proof-of-concept approach for elucidating interactions between various cell types and SF as well as demonstrating an OA-targeted potency assay for evaluating cell therapies. Together, the evidence from this exploratory study yields new information about molecular features present in pdSF that may function as critical attributes of knee OA severity and supports the use of a simSF product as an *in vitro* tool to advance OA research and development of candidate therapies to treat knee OA.

2. Methods

2.1. Ethical Statement

The Institutional Review Board (IRB) at the Georgia Institute of Technology issued a waiver (H19004) as no studies with human subjects were performed at the Georgia Institute of Technology for the present study. This study used de-identified samples from participants enrolled in the MILES clinical trial (NCT03818737) which was approved by the Western IRB, Emory University IRB, and Duke University IRB (IRB001080460). All participants provided written informed consent, and the clinical trial design for the MILES trial was performed independently of the present study. Participant samples used for the present study were chosen by Marcus Center for Therapeutic Cell Characterization and Manufacturing staff based on the availability of samples that were in excess of the planned investigations of the MILES clinical trial. This study was in compliance with all ethical requirements. The design of the study was exploratory, aimed at identifying potential indicators of knee Osteoarthritis correlated to pre-determined KL scores.

2.2. Hyaluronidase Treatment of pdSF

Vials of pdSF (n = 36) and a reference SF were thawed at room temperature and then centrifuged at 1000×g for 10 minutes. For each pdSF, 500 µL of supernatant was transferred to microcentrifuge tubes and incubated with 500 µL 4 mg/mL hyaluronidase (Sigma-Aldrich, St. Louis, MO) solution (50% v/v) for 15 minutes at 37˚C. Samples were vortexed for 5 seconds and then incubated for an additional

15 minutes at 37˚C. Samples were then centrifuged at 1000×g for 5 minutes and supernatants were collected and directly used in Luminex assays.

2.3. SF Characterization Using Luminex™ Assay

Hyaluronidase-treated pdSF samples (n = 36) were analyzed using Invitrogen™ Cytokine 30-Plex Human Panel Luminex™ (LHC6003M, Thermo Fisher Scientific, San Jose, CA) according to the manufacturer's instructions. Briefly, lyophilized standards were reconstituted and serially diluted to prepare 8 working standards. Luminex™ plates containing magnetic antibody-coated beads were washed after which standards (2 technical replicates prepared) or samples of pdSF (4 technical replicates prepared) were added to the wells for overnight incubation at 4˚C under mild agitation and protected from light. Using a magnetic 96-well separator, samples were decanted, washed twice, and incubated with biotinylated detector antibody for 1 hour at room temperature under mild agitation and protected from light. Using a magnetic separator, Luminex™ plates were then decanted, washed twice, and then incubated with streptavidin-RPE solution for 30 minutes at room temperature under mild agitation and protected from light. Next, the Luminex™ plates were washed three times using the magnetic separator and samples were analyzed using Luminex™ xMAP™ technology on a Bio-plex 200 system (Bio-Rad) to quantify cytokines concentrations.

2.4. Total Protein Assay

Total protein of neat pdSF samples (n = 36) was measured using Pierce™ BCA Protein Assay Kit according to manufacturer's instruction using the microplate procedure. Albumin standards were prepared by serial dilutions and added to wells of a 96-well plate (2 technical replicates prepared). pdSF samples were diluted 1:10 in PBS and then added to the wells of a 96-well plate (3 technical replicates prepared). Wells containing standards and pdSF were incubated with working reagent for 30 minutes at 37˚C. Following incubation, plates were allowed to cool for 5 minutes and then read using a standard plate reader under 562 nm absorbance.

2.5. Chondroitin Sulfate and Keratan Sulfate Assay

Hyaluronidase-treated pdSF samples (n = 6) were analyzed for chondroitin sulfate and keratan sulfate using commercially available ELISAs (Aviva Systems Biology) according to the manufacturer's protocols.

2.6. Rheological Analysis for Viscoelastic Properties

Neat pdSF samples (n = 17) were thawed and centrifuged to remove any cells or debris. Samples were then directed tested using 50mm cone-and-plate 1˚ attachment (Anton Paar MCR302). An amplitude sweep of pdSF was initially run to determine a strain % within the linear range. At a constant strain, each sample was tested via frequency sweep from 0.1 to 100 rad/sec.

2.7. Hyaluronic Acid Degradation Analysis and Classification

Neat pdSF samples (n = 24) that did were thawed, diluted 1:10 in PBS, and electrophoresed through 1.0% agarose gel. For each agarose gel, non-OA SF from 2 different donors (Articular Engineering, IL) were used as standards for non-degraded HA (e.g. 1.5 MDa and higher). In addition, varying amounts of 2.5 MDa HA (Creative PEGWorks, NC) and MW ladders (Echelon Biosciences, UT) were included on agarose gel to demonstrate linear range and size of HA quantification using 0.0025% Stain-All (Millipore-Sigma, Burlington, MA). All SF were stained and analyzed on 3 different gels and HA scores from each gel were averaged. simSF was prepared and analyzed similar to non-OA SF and pdSF.

Classification of HA was as follows: Score 1, intact HA stained-intensity (1.5 MDa and higher) was similar to non-OA SF with no sign of degradation (less than 1.5 MDa); Score 2, slight reduction of intact HA stained-intensity relative to non-OA SF with some sign of degradation; Score 3, decreased intact HA stained-intensity relative to non-OA SF (50% - 80%) with degradation; Score 4, HA was marginally detected on agarose gel (<20%). Scoring of all samples was done by the same blinded and trained observer to ensure consistency. pdSF samples and simSF were randomly arranged on a gel, except for non-OA SF samples, MW ladders, and 2.5 MDa HA standards. The observer was not privy to other SF assessments and analysis until complete submission of HA analysis for all pdSF and simSF.

2.8. Isolation and Expansion of BM-MSCs

Cryopreserved bone marrow aspirate concentrate (BMAC) was collected from four subjects in the MILES clinical trial and used for the isolation and expansion of bone marrow-derived mesenchymal stromal (BM-MSCs). Briefly, cryopreserved BMAC was thawed, washed, and counted to prepare 1×10^6 nucleated cells in 2 mL of isolation media (PRIME-XV MSC Expansion XSFM media (Fujifilm Irvine Scientific, Santa Ana, CA) supplemented with 1% PLTGold human platelet lysate (Millipore-Sigma) and 1% Penicillin-Streptomycin (Thermo Fisher Scientific) and plated into individuals wells in 6-well plates. After 24 hours, each well was washed twice with PBS to remove nonadherent cells, and then 2 mL isolation media was added to the adherent cells. Adherent cells were expanded for up to 14 days in a humidified incubator at 37˚ and 5% CO_2 with media changes every 3 - 4 days. Next, the cells were washed and harvested as passage (P) 0 BM-MSCs by incubation with TrypLE™ Express Enzyme (1X), no phenol red (Thermo Fisher Scientific) for 5 minutes at 37˚C and 5% CO_2. The cells were collected, neutralized with isolation media, and centrifuged at 300×g for 5 minutes. The supernatant was discarded and then cells were resuspended in isolation media and counted. The cells were further expanded to P1 in T-75 culture flasks (Corning®, Corning, NY) at 1×10^3 cells/cm^2 in serum-free media (PRIME-XV MSC Expansion XSFM media) for 4 - 5 days. P1 cells were harvested as previously described. P1 cells, now referred to as BM-MSCs, were cryopreserved in CryoStor10® (STEMCELL Technologies, Vancouver, Canada) at a concentration of 1.0×10^6 cells/mL. For expansion

to P2, P1 BM-MSCs were thawed, counted, and then plated in Corning ® CellBIND® T225 flasks (Corning) at 1×10^3 cells/cm^2 in serum-free media and cultured no longer than 5 days in a humidified incubator with 5% CO_2. P2 BM-MSCs were washed, harvested, and then cryopreserved as previously described until used for *in vitro* testing.

2.9. OA-Targeted Potency Assay

P2 BM-MSCs from four subjects (referred to as donors in the assay) were thawed, counted, and then prepared at a concentration of 8.0×10^5 cell/mL in serum-free media (PRIME-XV MSC Expansion XSFM media). Using a 96-well plate, 100 µL of cell suspension was plated into each well (4 technical replicates prepared) and then placed in a humidified incubator set to 37˚C and 5% CO_2. After 24 hours, 20% pdSF or 20% simSF was prepared in serum-free media, and 100 µL of either pdSF or simSF was added to the cells in each well designated for pdSF or simSF exposure, resulting in exposure of the cells to a final formulation of 10% pdSF or 10% simSF. 100 µL of XSFM alone was also added to cells designated as basal media controls. The plate was placed in a humidified incubator for 24 hours, and then conditioned media was collected and stored at −20˚C for Luminex™ analysis. The Invitrogen™ Cytokine 30-Plex Human Panel Luminex™ was used to analyze the conditioned media as described above in the methods for SF characterization using Luminex™ Assay.

2.10. *In Vitro* Macrophage Assay

Human THP-1 monocytes (TIB-202, ATCC, Manassas, VA) were thawed, counted and expanded in 20% heat-inactivated (HI) fetal bovine serum (FBS; Hyclone), 1% Penicillin/Streptomycin (P/S; Sigma), 0.05 mM β-mercaptoethanol (BME, Sigma) supplemented RPMI-1640 medium (ATCC) in T-25 suspension flasks, placed upright in a humidified incubator set to 37˚C and 5% CO_2. Using a CellBIND® 96-well plate (Corning, Corning, NY), harvested cells were plated at a seeding density of 105 cells/well in differentiation media (1% HI FBS, 100 ng/mL phorbol 12-myristate 13-acetate, 1% P/S, RPMI-1640) and left to attach and differentiate to naïve macrophages over 48 hr at 37˚C and 5% CO_2. After this time, the plate was centrifuged at 300×g for 5 min to settle loosely adherent cells and media was aspirated carefully to avoid removing cells. Media was changed to 1% FBS, P/S, RPMI-1640 supplemented with lipopolysaccharide (LPS from *E. coli*, 100 ng/mL, Sigma-Aldrich) and interferon gamma (IFNγ, 100 ng/mL, Peprotech, Rocky Hill, NJ) with or without the addition of 10% simSF or 10% pdSF. The plate was then incubated for 24 hours at 37˚C and 5% CO_2. Conditioned media supernatant was removed to a 96-well plate and stored at −20˚C prior to Luminex™ analysis as described above in the methods for SF characterization using Luminex™ Assay.

2.11. Machine Learning by Symbolic Regression

A tabular matrix was created with patient information and associated pdSF char-

acterization data as described in Supplementary Table S1. Symbolic regression was performed to identify top features, or potential predictors, correlative to KL score or HA electrophoresis grade using DataModeler software (Evolved Analytics, Rancho Santa Fe, CA). Using all inputs (*i.e.*, available patient information and pdSF characterization data), DataModeler generated symbolic regression models and selected the best fit models which are those possessing the greatest accuracy (R^2 value) and lowest complexity as identified by a Pareto front. The fittest models were then analyzed to identify top variables using the Variable Presence and Variable Combinations functions. Predictive features of KL score or HA electrophoresis grade were selected based on the highest percentage of presence in coinciding models identified by Variable Combinations function. This same approach was performed to identify top variables from either Luminex™ (Lumx) data only or patient information only correlated to KL score or HA electrophoresis grade.

2.12. Analysis

Raw data from Luminex™ assays were imported into JMP 15 software for analysis and to generate Z-scores. Heat maps of Z-scores, violin plots, and bar and line graphs were created using GraphPad Prizm software v10. Data was represented as the mean ± standard error of the mean.

3. Results

3.1. OA pdSF Patient Information and Data Distribution

The distribution of de-identified OA patient information and pdSF samples data is shown in Supplementary Figures 1(A)-(F), and the record of related patient information and characterization performed for each pdSF sample is compiled in Supplementary Table S1. Ages ranged from 50 to 70 years with an average age of 60.0 ± 5.3 years. The average BMI was 29.4 ± 5.2 which ranged from 21.6 to 42.9. KL scores of OA patients were used as model outputs and were reported as KL 2 (n = 9), KL 3 (n = 18), and KL 4 (n = 14). An unequal distribution of patients' sex, *i.e.* females (n = 16) to males (n = 25), resulted from the pdSF sample selection based on available volume for characterization assays. An unequal distribution of KL scores also resulted among each sex. Of the females, the average age was 59.6 ± 5.0 years old, BMI was 27.9 ± 5.5, and KL score distribution was 4 OA patients with KL 2, 9 with KL 3, and 3 with KL 4. For the males, the average age was 60.0 ± 5.3, BMI was 30.4 ± 4.9, and KL score distribution was 5 OA patients with KL 2, 9 with KL 3, and 11 with KL 4 (Supplementary Figure S1(A), Supplementary Figure S1(B), Supplementary Figure S1(C)).

Additional pdSF information recorded at the time of collection was the total volume of pdSF collected and the nucleated cell concentration in pdSF (Supplementary Table S1). Less than 20 mL was collected from afflicted OA knees for most of the pdSF samples (Supplementary Figure S1(D)) and most pdSF collected had little to no cells present (Supplementary Figure S1(F)). The color of pdSF was evaluated using a color key (Supplemental Figure S1(G)) which was recorded

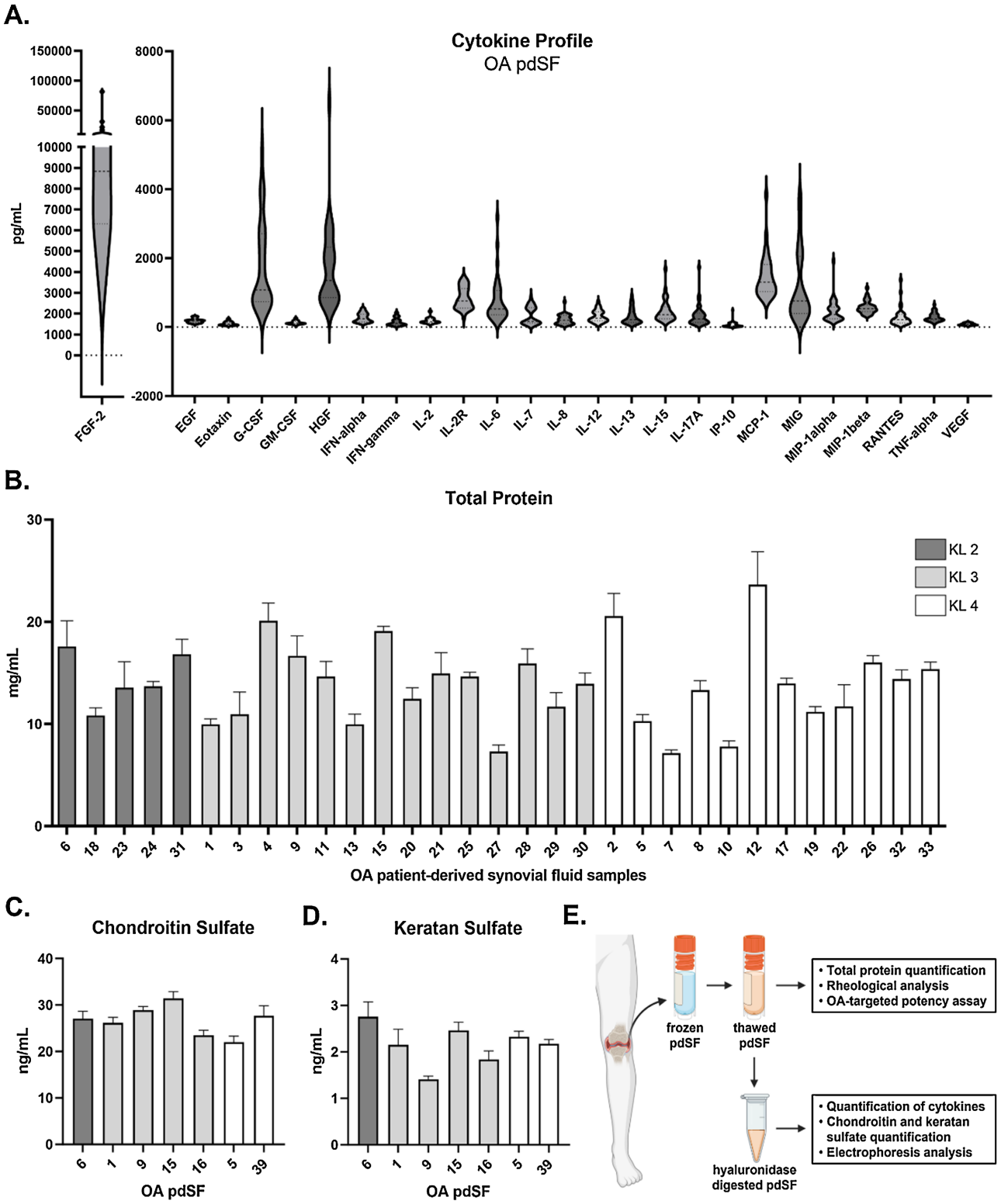

Figure 1. Characterization of pdSF composition. (A) The cytokine profile of pdSF samples (n = 36) included 24 cytokines present in all pdSF samples. FGF-2 which was measured with the highest concentration in 18 of 36 pdSF samples. Violin plots showed the distribution and standard deviation of pdSF samples for each cytokine. (B) The total protein concentration of each pdSF sample (n = 36) arranged by KL score. (C), (D) Chondroitin sulfate and keratan sulfate concentrations measured in pdSF (n = 7) and arranged by KL score.

after a freeze-thaw cycle in which a close to parabolic distribution around color 4 was seen among all pdSF samples (Supplementary **Figure S1(E)**).

3.2. Protein Composition of pdSF Shows High Variabilities and No Apparent Trend Related to KL Score

Twenty four (out of 30) cytokines were detected in all 36 pdSF by Luminex™ analysis. The most abundant cytokine detected was basic fibroblast growth factor, or FGF-2, which was measurable in 18 of the 36 pdSF with the remaining samples missing data as a result of being above the range of detection. Of these pdSF, the variability of FGF-2 among the sample measured was represented by the wide range in concentration from 3321.4 to 81,509.7 pg/mL averaging 14,401.6 ± 18,082.2 pg/mL. The top cytokines present in all pdSF samples included 6 cytokines with markedly high average concentrations including hepatocyte growth factor (HGF; 1657.3 ± 1182.4 pg/mL), granulocyte-colony stimulating factor (G-CSF; 1746.2 ± 1261.4 pg/mL), monocyte chemoattractant protein-1 (MCP-1; 1433.5 ± 634.0 pg/mL), monokine induced by interferon-gamma (MIG; 1130.9 ± 1027.2 pg/mL), interleukin-2R (IL-2R; 778.9 ± 365.1 pg/mL), and interleukin-6 (IL-6; 719.0 ± 653.9 pg/mL; **Figure 1(A)**).

The total protein content of pdSF (n = 31) was measured with a combined average of 13.9 ± 3.9 mg/mL. The total protein content ranged between 7.13 to 23.6 mg/mL with no apparent trend related to KL score (**Figure 1(B)**). Similarly, CS and KS were glycosaminoglycans measured in pdSF (n = 7) with average combined concentrations of 26.7 and 2.2 ng/mL, respectively. CS ranged from 22.0 to 31.5 ng/mL, and KS ranged from 1.4 to 2.8 ng/mL (**Figure 1(C)** and **Figure 1(D)**). Rheological properties were measured as the viscosity, storage modulus, and loss modulus for pdSF (n = 18). As the shear rate increased from 0.1 to 100 s^{-1}, the viscosities of all pdSF samples decreased with corresponding viscosity curves. At 0.1 s^{-1}, the pdSF with the highest viscosity measured 3622.8 ŋ, the lowest viscosity of 69.4 ŋ, and combined average of all pdSF was 1552.4 ŋ (**Figures 5(A)-(C)**).

3.3. Electrophoresis Reveals Degradation of HA

The HA content of 24 pdSF samples was assessed using Stained-All agarose electrophoresis (Bowman *et al.*, 2011) (**Figure 2(A)**). To provide semi-quantification assessment of HA, a classification system was developed to score HA content from 1 (normal) to 4 (severe degradation of HA). This classification system relied on using non-OA SF as reference on the agarose gel and HA molecular weight ladders to delineate degraded (<1.5 MDa) from intact (>1.5 MDa) HA. Intact HA in pdSF was ~4 MDa as assessed on agarose gel, since pdSF HA band ran slower than the 2.5 MDa HA standard (from Creative PEGWorks) and faster than the 6 MDa band (Select-HA MegaLadder from Echelon Biosciences) (**Figure 2(B)**). Of the 24 pdSF samples assessed, 6 showed a slight decrease in HA content (score of 2), 11 exhibited decreased HA content and evidence of degradation (score of 3), and 7 had almost no HA in their SF (score of 4), and non-OA controls were classified as a

score of 1 (Figure 2(C)).

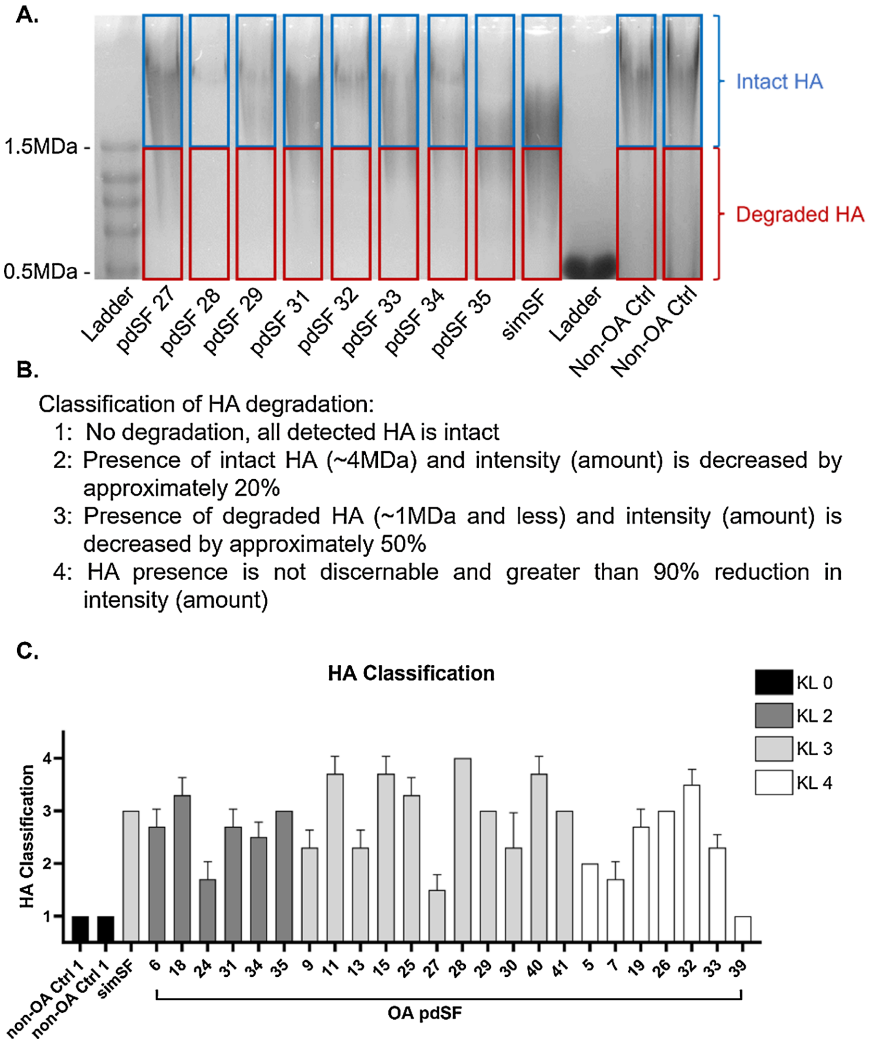

Figure 2. Electrophoresis analysis categorized the degradation of HA in pdSF. (A) Image of an agarose gel stained with Stains = all to represent HA and degradation. (B) An HA classification system was developed to differentiate between intact and degraded HA. (C) HA electrophoresis grade results of pdSF analysis using the HA classification system arranged by KL score.

3.4. Comparability of Responses of Macrophages to pdSF and simSF

THP-1 macrophages (THP-1M) were induced with LPS (+LPS) to a pro-inflammatory M1-like phenotype to mimic local macrophages in OA knees. Groups of THP-1M + LPS were then exposed to either simSF (+simSF) or pdSF (+pdSF) to elicit secretory responses for comparisons among all macrophage groups. THP-1M + LPS group (no exposure) secreted the highest levels of detected cytokines including IL-1β, IL-12, IL-1RA, IL-6, IL-7, MIP-1α, MIP-1β, and VEGF compared to those exposed to simSF (THP-1M + LPS + simSF) or pdSF (THP-1M + LPS + pdSF). Macrophages exposed to simSF or pdSF secreted comparably less IL-1β,

IL-7, MIP-1β, and VEGF than those not exposed (THP-1M + LPS). Differences in cytokine secretion between the macrophage exposure groups were measured between IL-10, IL-12, IL-6, IL-8, IP-10, MCP-1, MIG, MIP-1α, and TNF-α and comparability was most evident in the secretion of IL-1RA, IL-2R, RANTES, and VEGF. As expected, the media control groups that did not contain macrophages had no presence of detected cytokines (**Figure 7(B)**).

3.5. SR Models Identify Potential Predictors of KL Score and Electrophoresis Grade

SR models were used to identify the top variables of KL score when all of the patient information and Luminex (Lumx) analysis of cytokines were allowed as potential inputs. From the 8903 models generated, 103 models achieved $R^2 \geq 85\%$ and were further evaluated to identify the variables most present in the top performing models (highest accuracy and lowest complexity). Three variables were present in greater than 80% of the top performing models: SF cell concentration (100%), SF volume collected (97%), BMI (84%), and two were greater than 50%, IL-6 (66%) and IL-17A (55%) (**Figure 3(A)**). Following a similar approach, SR models were used to identify the top variables of HA electrophoresis grade when all inputs were allowed. From the 8053 models generated, 1643 achieved $R^2 \geq 95\%$. Interestingly, SF cell concentration (100%), SF volume collected (100%), and total protein concentration (98%) were identified as top variables along with MIG (85%) and GM-CSF (74%) (**Figure 3(B)**).

To target key cytokines in pdSF that are indicative of OA severity, SR models were generated with only Luminex data (Lumx) to identify top cytokines correlative to either KL score or HA electrophoresis grade. The cytokines identified as top variables correlative to KL score ($R^2 \geq 60\%$) were Eotaxin (100%), IL-8 (100%), IL-13 (100%), and MCP-1 (87%) (Supplementary **Figure S2(A)**). Top cytokines identified as top variables correlative to HA electrophoresis grade ($R^2 \geq 90\%$) were IL-6 (100%), IL-17A (87%), MIG (72%), HGF (67%) and GM-CSF (55%) (Supplementary **Figure S2(B)**). Using only patient information and pdSF attributes (*i.e.*, sex, age, BMI, color SF volume collected, SF cell concentration), SR models ($R^2 \geq 70\%$) identified SF cell concentration (100%), color (100%), BMI (98%), and SF volume collected (94%) as the top variables correlated to KL score (Supplementary **Figure S3(A)**). Using these same inputs to identify top variables correlative to electrophoresis grade, SR models ($R^2 \geq 90\%$) identified age (100%), BMI (100%), SF Volume collected (100%) and SF cell concentration (100%) (Supplementary **Figure S3(B)**).

3.6. Key Components and Viscoelastic Properties of pdSF Informed the Development of simSF

The characterization of pdSF identified key components, e.g. cytokines, that were present in high abundances in all samples and provided relative physiological concentrations that were used to inform development of prototypes that were tested to create the final simSF product (**Figure 4(A)**). A stepwise procedure was

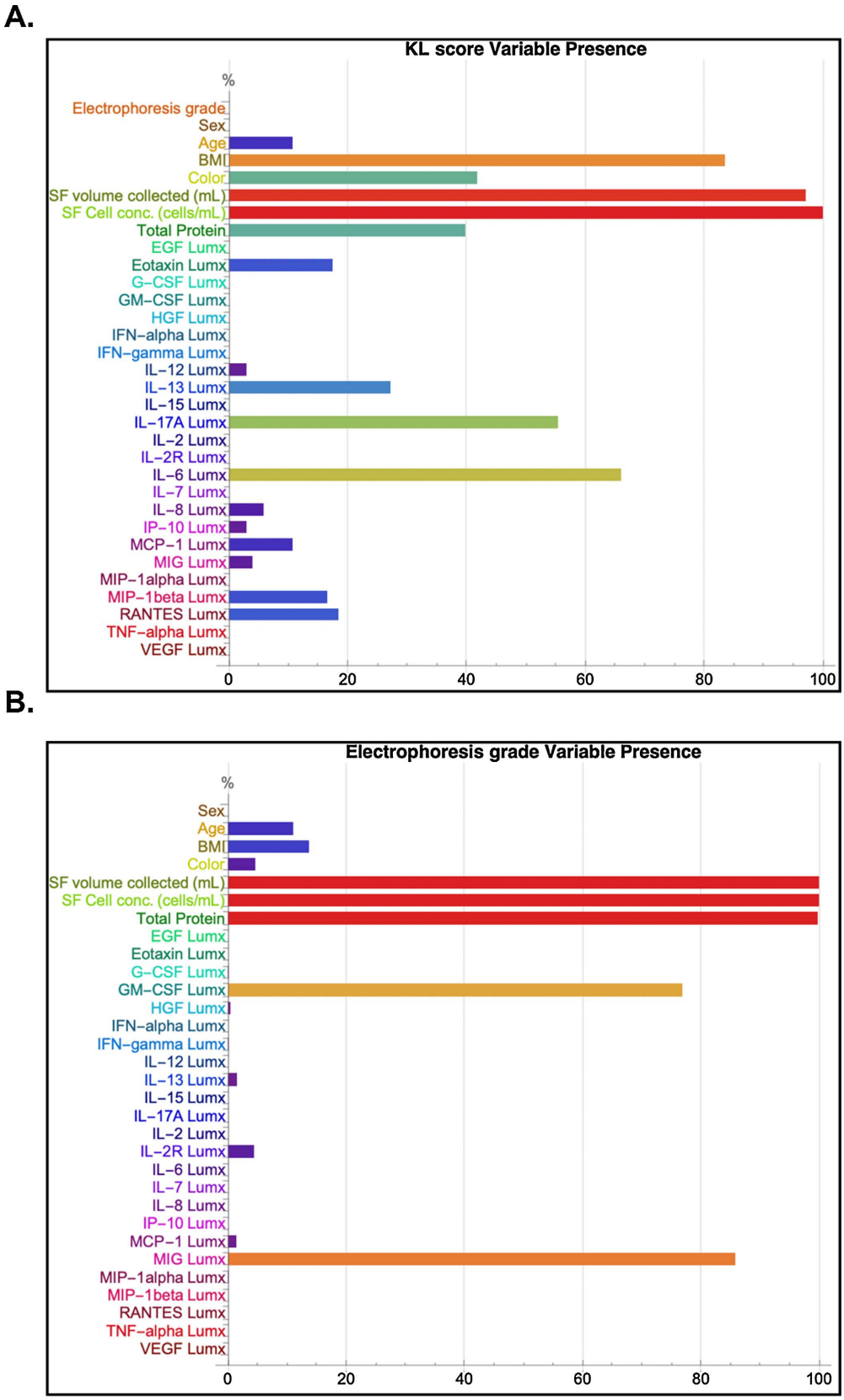

Figure 3. pdSF sample information and characterization data were correlated to KL score to identify top features correlative to KL score.

A.

Component	Amount	Purpose
Phosphate buffered saline (PBS), no Ca^{2+} and Mg^{2+}	---	Physiologically relevant vehicle for cells
Human serum albumin	25 mg/mL	Most abundant large protein in synovial fluid
Basic Fibroblast Growth Factor (bFGF)	120 ng/mL	Most abundant cytokine present in all pdSF samples
Granulocyte-Colony Stimulating Factor (G-CSF)	30 ng/mL	Most abundant cytokine present in all pdSF samples
Hepatocyte Growth Factor (HGF)	26 ng/mL	Most abundant cytokine present in all pdSF samples
Monocyte Chemoattractant Protein-1 (MCP-1)	19 ng/mL	Most abundant cytokine present in all pdSF samples
Monokine Induced by Interferon-Gamma (MIG)	18 ng/mL	Most abundant cytokine present in all pdSF samples
Chondroitin Sulfate (CS)	4 µg/mL	Potential biomarker of OA [ref]
Keratan Sulfate (KS)	20 µg/mL	Potential biomarker of OA [ref]
Low MW hyaluronic acid	100 µg/mL	Provides inflammatory stimulus
High MW hyaluronic acid	3 mg/mL	Provides viscoelastic properties

B.

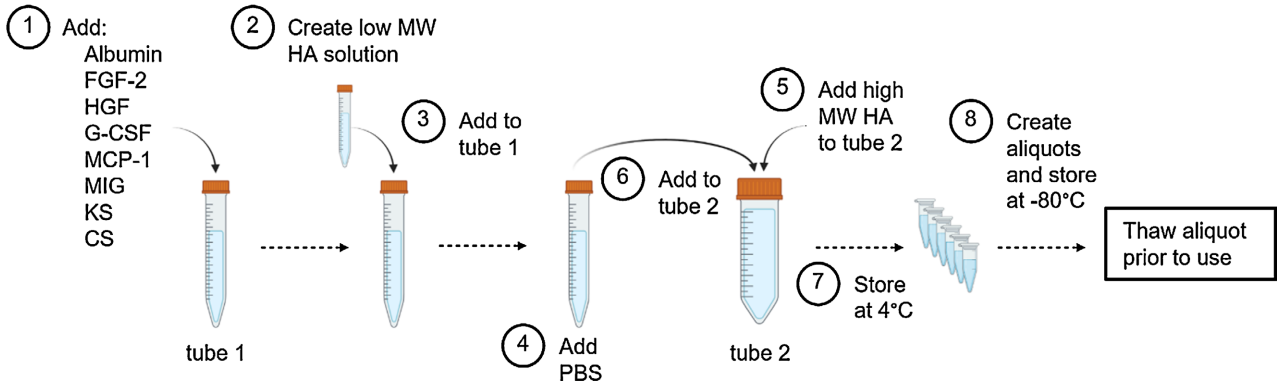

Figure 4. Development of simSF. (A) Key components determined by pdSF characterization were chosen and included in the simSF at relative physiological concentrations. (B) Stepwise protocol for developing simSF.

performed to create a solution with comparable viscoelastic properties as pdSF (Figure 4(B)). Rheological measurements demonstrated equivalent viscosity, storage modulus, and loss modulus between the final simSF product and the pdSF samples with the highest and lowest measurements (Figure 5).

3.7. simSF Elicited Similar Secretory Responses of BMAC as pdSF

The OA-targeted potency assay was developed to evaluate donor-specific secretory responses of BMAC when exposed to an OA-like environment. Moreover, this assay's purpose was to demonstrate the use of pdSF and simSF in an *in vitro* assay to help predict possible effects of BM-MSCs following therapeutic administration of BM-MSCs into OA knees. The assay was performed according to the schematic shown in Figure 6(A) in which BM-MSCs were exposed to either pdSF or simSF for 24 hours prior to collection and analysis of the conditioned media containing secreted analytes.

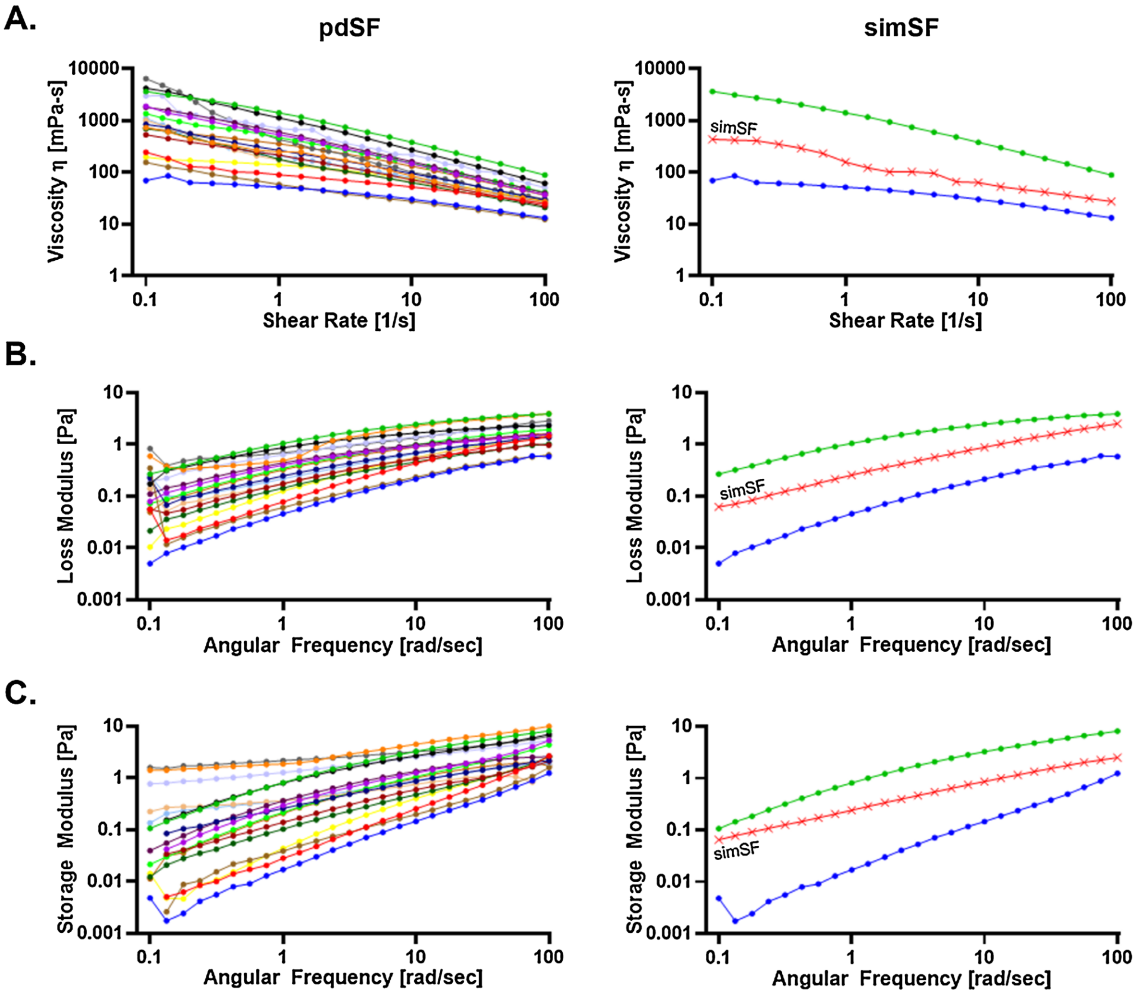

Figure 5. Similar viscoelastic properties of simSF and pdSF. A. Viscosity, B. Loss Modulus, and C. Storage Modulus results of pdSF (n = 18; left) and simSF. For simSF results, the maximum (green line) and minimum (blue line) results from pdSF measurements are shown for comparison to simSF (red line).

BM-MSCs derived from the BMAC from four OA donors were evaluated in the OA-targeted potency assay and designated to 3 conditions: 1) exposed to media only, 2) exposed to media containing simSF, or 3) exposed to media containing pdSF (representative sample from one OA donor). Results show measurable responses in the secretion from all BM-MSCs based on fibroblast growth factor-β (FGF-β), hepatocyte growth factor (HGF), interleukin-2-receptor (IL2-R), interleukin-6 (IL-6), interleukin-8 (IL-8), MCP-1, and vascular endothelial growth factor A (VEGF-A). Heatmap results generated from the Z-scores suggest similar secretory responses from donor BM-MSCs exposed to simSF compared to those exposed to pdSF (Figure 6).

3.8. Comparability of Responses of Macrophages to pdSF and simSF

THP-1 macrophages (THP-1M) were induced with LPS (+LPS) to a pro-inflammatory M1-like phenotype to mimic local macrophages in OA knees. Groups of

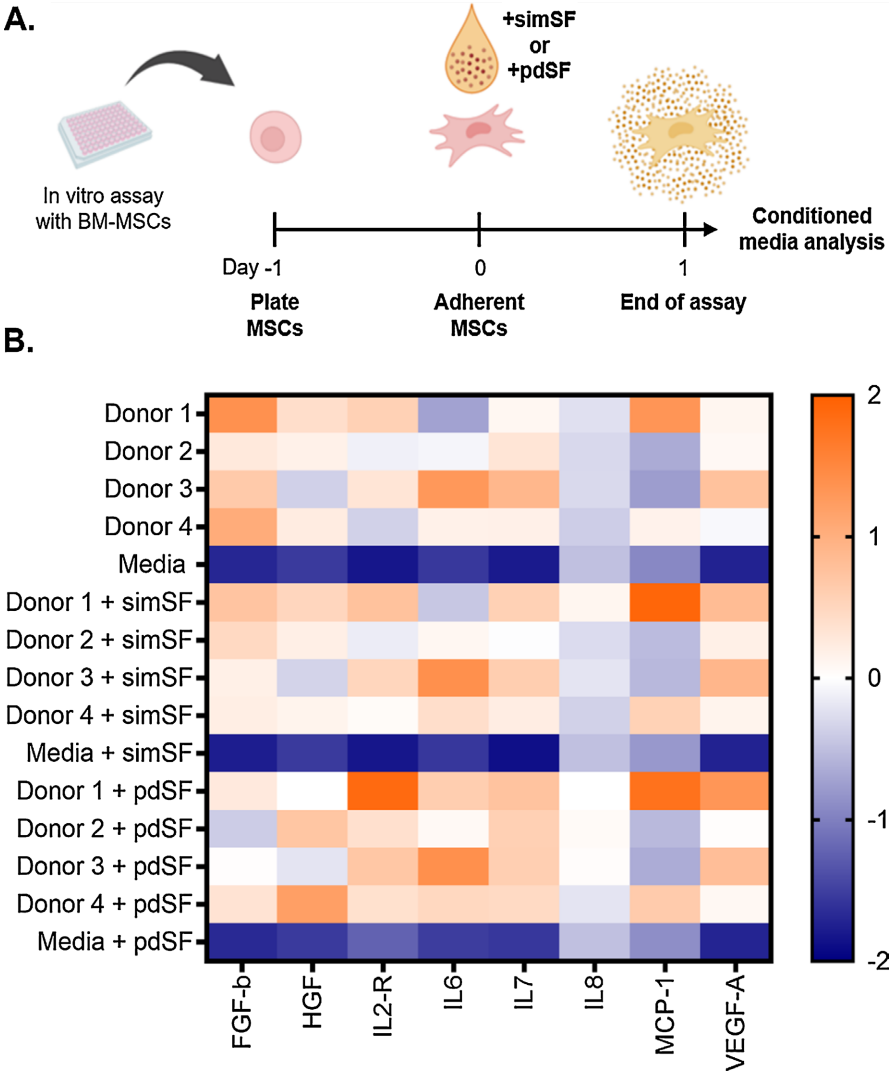

Figure 6. BM-MSC responses to pdSF and simSF in OA-targeted potency assay. A. Schematic of the assay workflow. B. Results shown as heatmap of the Z-scores from testing 3 donors of BM-MSCs in basal culture conditions, with exposure to simSF, and with pdSF. Media controls were included.

THP-1M + LPS were then exposed to either simSF (+simSF) or pdSF (+pdSF) to elicit secretory responses for comparisons among all macrophage groups. THP-1M + LPS group (no exposure) secreted the highest levels of detected cytokines including IL-1β, IL-12, IL-1RA, IL-6, IL-7, MIP-1α, MIP-1β, and VEGF compared to those exposed to simSF (THP-1M + LPS + simSF) or pdSF (THP-1M + LPS + pdSF). Macrophages exposed to simSF or pdSF secreted comparably less IL-1β, IL-7, MIP-1β, and VEGF than those not exposed (THP-1M + LPS). Differences in cytokine secretion between the macrophage exposure groups were measured between IL-10, IL-12, IL-6, IL-8, IP-10, MCP-1, MIG, MIP-1α, and TNF-α and comparability was most evident in the secretion of IL-1RA, IL-2R, RANTES, and VEGF. As expected, the media control groups that did not contain macrophages had no presence of detected cytokines (**Figure 7(B)**).

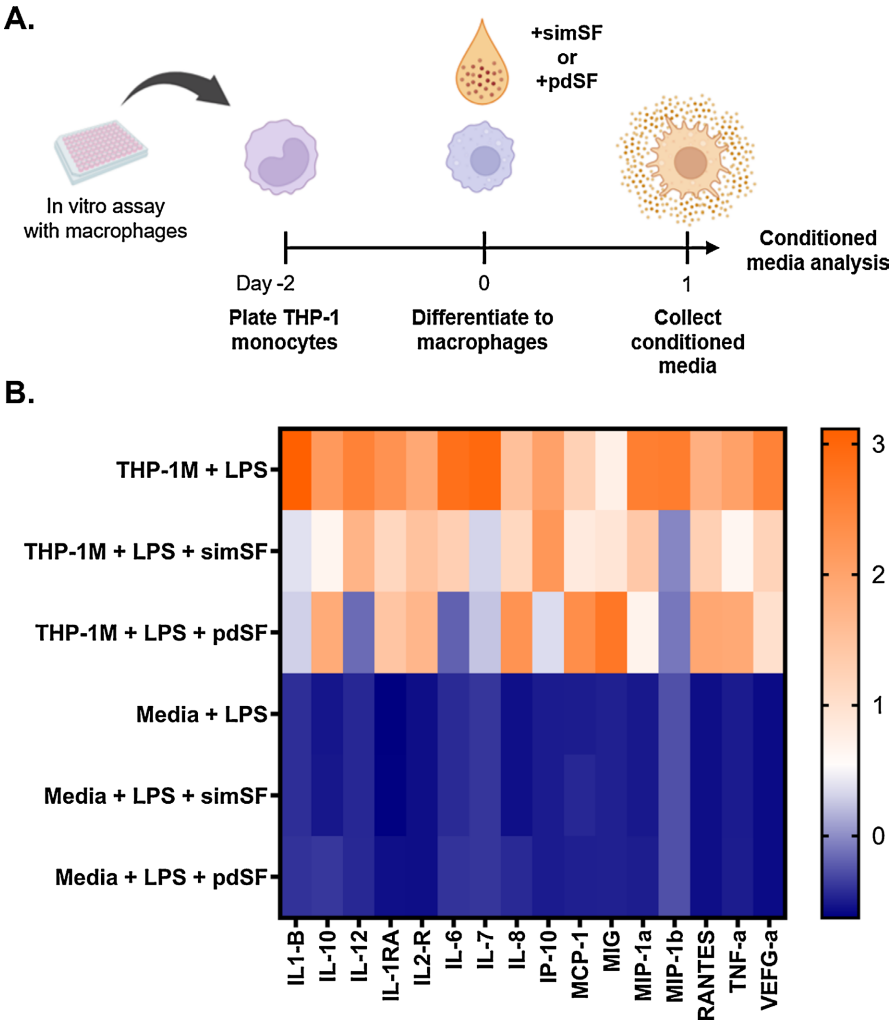

Figure 7. simSF mimics cellular responses of macrophages to pdSF *in vitro*. (A) Schematic of the assay workflow. (B) Results shown as heatmap of the Z-scores from testing THP-1 macrophages in basal culture conditions, with exposure to simSF, and with pdSF. Media controls were included.

4. Discussion

Investigations to better understand knee OA severity demonstrate a need to uncover correlative features present in pdSF that have the potential to aid in the development of effective and targeted treatments. In this study, we used common laboratory assays as well as novel assays to elucidate the molecular and physiological properties of pdSF. We combined deep characterization with patient information related to the pdSF to create input features that were correlated to KL score using SR models to identify top features of OA severity. A similar approach was performed to identify top features associated with HA degradation, which is a defining pathological result of OA, using a novel electrophoresis-based grading system. SR based machine learning modeling is an advanced tool used to identify correlations and can perform predictions from fitting large amounts of data to mathematical models based on accuracy and complexity. In past studies,

DataModeler's SR models have been used to predict potency and optimize critical quality parameters from multiomics data of cell therapy production [28]-[31]. Here, DataModeler's SR models used features that were related to the OA patient (e.g., age, sex, BMI), pdSF data collected at the clinical site (e.g., color, total volume collected, cell concentration), and characteristics of pdSF using common laboratory methods (e.g., total protein concentration, cytokines,).

Sex, age, and BMI are known risk factors of OA [32] which were input data included in this study. Using all input data available in Supplementary **Table S1** for correlations to KL score, results from SR models identified top features (*i.e.*, features present in >80% of all SR models) as the cell concentration of the pdSF, total volume collected of pdSF, and BMI (**Figure 3(A)**). HA electrophoresis grade was hypothesized to correlated to KL score, however, based on the SR models no correlation was identified which led this study into taking separate approaches to identify correlations to either KL score or HA electrophoresis grade. For correlation to HA electrophoresis grade which represents the amount of hyaluronic degradation detected in pdSF, top features identified by SR models were the total volume collected of pdSF, cell concentration of the pdSF, total protein, and MIG (**Figure 3(B)**). When inputs were limited to the patient information and pdSF data collected at the clinical site, the top features correlative to KL score present in over 94% of SR models were the color of pdSF, the cell concentration, the total volume collected, and BMI, and the top features correlative to HA electrophoresis grade (*i.e.*, amount of HA degradation) present in 100% of SR models were age, BMI, the cell concentration, and total volume collected (Supplementary **Figure S3(A)** and **Figure S3(B)**). These top features can be data collected at clinical sites with little need for equipment besides a cell counter. More importantly, these features could potentially be used to assist in defining the severity of OA or support the diagnosis based on KL score.

Top features from the characterization of pdSF using common laboratory methods (e.g., Luminex) are pertinent to understanding the pathological underpinnings of knee OA severity and the development of targeted therapies. Of the cytokines quantified in this study, the top features correlative to KL score identified were Eotaxin, IL-13, IL-8, and MCP-1. Together, these molecules are known to play roles in inflammation corroborating the low-grade inflammatory signaling present in the OA knee milieu [33]-[36]. When the cytokine profile of pdSF was used to correlated to HA degradation, SR models identified IL-6, IL-17A, MIG, HGF and GM-CSF in over 50% of the models. These cytokines play distinct and often interconnected roles in regulating the immune system and inflammation in various diseases [37]-[39]. These results are also informative for a cost-effective way to study knee OA severity and pathology by customizing panels of these top features identified from deep characterization. The majority of these cytokines are known pro-inflammatory signals mediating cell-cell interactions in the local milieu, further supporting the inflammatory processes that underpin knee OA [32] [38]. These results also identify potential targets of potential mechanisms of action

by developed treatments. Independent external validation with larger cohorts will be required before any predictive performance claims can be generalized.

The development of a simSF product will enable research into candidate treatments and their potential outcomes for knee OA independent of access to pdSF. pdSF characterization informed the development of the simSF and results demonstrated that the simSF closely mimicked a representative pdSF. simSF contained average concentrations of the most abundant proteins found in pdSF (**Figure 1(A)**, **Figure 4(A)**) as well as proposed biomarkers of OA in pdSF related to degradation (*i.e.*, CS, KS; **Figure 1(C)**, **Figure 1(D)**, **Figure 4(A)**). Additionally, simSF contained low MW HA which is present in OA pdSF from degradation and is known to stimulate local immune cells to promote pro-inflammatory activities [40]. The concentration of high MW HA was determined by the viscoelastic properties of the pdSF to which simSF results were comparable. simSF comparability to pdSF was further supported by the results generated from the HA degradation method using electrophoresis which classified simSF similar to the pdSF samples that were measured (**Figure 2(C)**).

To demonstrate the utility of simSF, we compared the results from the OA-targeted potency assay of BM-MSC cell secretory responses from multiple donors elicited between simSF and pdSF. Results showed eight cytokines quantified in media following 24-hour exposure of BM-MSCs to simSF or pdSF. Similar trends were seen in the cytokine profiles released by cells from the same donor in simSF or pdSF in which the majority of the cytokines were increased upon simSF or pdSF exposure. A recent study published by our group demonstrated the utility of simSF in a novel on-chip 3D potency assay for predicting clinical outcomes for OA following cell therapies. Results from this study demonstrated that *in vitro* potency assays can serve as promising tools for proposing therapeutic efficacy of treatment candidates [41]. Additionally, we were able to demonstrate that simSF elicited secretory responses from macrophages similar to pdSF in the assay developed to recapitulate the OA environment. Compared to the controls which were macrophages induced to the M1 phenotype by the addition of LPS, simSF and pdSF modulated the secretory responses of M1-induced macrophages and this was observed in the levels of several cytokines and growth factors. These assays can be valuable tools used for OA research in which candidate therapies can be screened *in vitro* and potential mechanisms of action can be identified.

This study provided new evidence for knee OA severity by comprehensively investigating pdSF. This evidence included the identification of critical attributes of knee OA in pdSF that were correlative to OA severity, characteristics of pdSF that supported the current understanding of knee OA, the development of a simSF product for *in vitro* testing, and *in vitro* assays developed to mimic an OA-like environment for testing candidate therapies for knee OA. Together, these advances and tools will enable innovative explorations into key pathological interactions and targeted approaches to treating knee OA.

Acknowledgements

We would like to thank the clinicians, faculty, and study coordinators for the MILES clinical trial who provided the samples of pdSF and BMAC. This work was supported by FDA (AWD-001738), The Billi and Bernie Marcus Foundation to the Marcus Center for Therapeutic Cell Characterization and Manufacturing (MC3M), the Georgia Research Alliance, the Georgia Tech Foundation, the National Science Foundation Engineering Research Center for Cell Manufacturing Technologies (NSF EEC 1648035), and Emory University.

Conflicts of Interest

TK is the CEO of Evolved Analytics LLC which provided DataModeler software to build symbolic regression models in this study. All the other authors declare no competing interests.

References

[1] Tamer, T.M. (2013) Hyaluronan and Synovial Joint: Function, Distribution and Healing. *Interdisciplinary Toxicology*, **6**, 111-125. https://doi.org/10.2478/intox-2013-0019

[2] Hui, A.Y., McCarty, W.J., Masuda, K., Firestein, G.S. and Sah, R.L. (2011) A Systems Biology Approach to Synovial Joint Lubrication in Health, Injury, and Disease. *WIREs Systems Biology and Medicine*, **4**, 15-37. https://doi.org/10.1002/wsbm.157

[3] Chou, C., Jain, V., Gibson, J., Attarian, D.E., Haraden, C.A., Yohn, C.B., *et al.* (2020) Synovial Cell Cross-Talk with Cartilage Plays a Major Role in the Pathogenesis of Osteoarthritis. *Scientific Reports*, **10**, Article No. 10868. https://doi.org/10.1038/s41598-020-67730-y

[4] Loeser, R.F., Goldring, S.R., Scanzello, C.R. and Goldring, M.B. (2012) Osteoarthritis: A Disease of the Joint as an Organ. *Arthritis & Rheumatism*, **64**, 1697-1707. https://doi.org/10.1002/art.34453

[5] Steenkamp, W., Rachuene, P.A., Dey, R., Mzayiya, N.L. and Ramasuvha, B.E. (2022) The Correlation between Clinical and Radiological Severity of Osteoarthritis of the Knee. *SICOT-J*, **8**, Article No. 14. https://doi.org/10.1051/sicotj/2022014

[6] Gao, F., Tian, J., Pan, H., Gao, J. and Yao, M. (2015) Association of CCL13 Levels in Serum and Synovial Fluid with the Radiographic Severity of Knee Osteoarthritis. *Journal of Investigative Medicine*, **63**, 545-547. https://doi.org/10.1097/jim.0000000000000150

[7] Zou, L., Liu, J. and Lu, H. (2018) Correlation of Concentrations of Activin A with Occurrence and Severity of Knee Osteoarthritis. *Journal of Musculoskeletal Neuronal Interactions*, **18**, 320-322.

[8] Liu, Y., Hou, R.Z., Yin, R.F. and Yin, W.T. (2015) Correlation of Bone Morphogenetic Protein-2 Levels in Serum and Synovial Fluid with Disease Severity of Knee Osteoarthritis. *Medical Science Monitor*, **21**, 363-370.

[9] Xu, Q., Sun, X., Shang, X. and Jiang, H. (2012) Association of CXCL12 Levels in Synovial Fluid with the Radiographic Severity of Knee Osteoarthritis. *Journal of Investigative Medicine*, **60**, 898-901. https://doi.org/10.2310/jim.0b013e31825f9f69

[10] Timur, U.T., Jahr, H., Anderson, J., Green, D.C., Emans, P.J., Smagul, A., *et al.* (2021) Identification of Tissue-Dependent Proteins in Knee OA Synovial Fluid. *Osteoarthri-*

tis and Cartilage, **29**, 124-133. https://doi.org/10.1016/j.joca.2020.09.005

[11] Peffers, M.J., McDermott, B., Clegg, P.D. and Riggs, C.M. (2015) Comprehensive Protein Profiling of Synovial Fluid in Osteoarthritis Following Protein Equalization. *Osteoarthritis and Cartilage*, **23**, 1204-1213. https://doi.org/10.1016/j.joca.2015.03.019

[12] Lindhorst, E., Vail, T.P., Guilak, F., Wang, H., Setton, L.A., Vilim, V., *et al.* (2000) Longitudinal Characterization of Synovial Fluid Biomarkers in the Canine Meniscectomy Model of Osteoarthritis. *Journal of Orthopaedic Research*, **18**, 269-280. https://doi.org/10.1002/jor.1100180216

[13] Balazs, E.A., Watson, D., Duff, I.F. and Roseman, S. (1967) Hyaluronic Acid in Synovial Fluid. I. Molecular Parameters of Hyaluronic Acid in Normal and Arthritic Human Fluids. *Arthritis & Rheumatism*, **10**, 357-376. https://doi.org/10.1002/art.1780100407

[14] Mateos, J., Lourido, L., Fernández-Puente, P., Calamia, V., Fernández-López, C., Oreiro, N., *et al.* (2012) Differential Protein Profiling of Synovial Fluid from Rheumatoid Arthritis and Osteoarthritis Patients Using LC-MALDI TOF/TOF. *Journal of Proteomics*, **75**, 2869-2878. https://doi.org/10.1016/j.jprot.2011.12.042

[15] Strauss, E.J., Hart, J.A., Miller, M.D., Altman, R.D. and Rosen, J.E. (2009) Hyaluronic Acid Viscosupplementation and Osteoarthritis: Current Uses and Future Directions. *The American Journal of Sports Medicine*, **37**, 1636-1644. https://doi.org/10.1177/0363546508326984

[16] Band, P.A., Heeter, J., Wisniewski, H.-., Liublinska, V., Pattanayak, C.W., Karia, R.J., *et al.* (2015) Hyaluronan Molecular Weight Distribution Is Associated with the Risk of Knee Osteoarthritis Progression. *Osteoarthritis and Cartilage*, **23**, 70-76. https://doi.org/10.1016/j.joca.2014.09.017

[17] Yamada, H., Miyauchi, S., Hotta, H., Morita, M., Yoshihara, Y., Kikuchi, T., *et al.* (1999) Levels of Chondroitin Sulfate Isomers in Synovial Fluid of Patients with Hip Osteoarthritis. *Journal of Orthopaedic Science*, **4**, 250-254. https://doi.org/10.1007/s007760050100

[18] Belcher, C., Yaqub, R., Fawthrop, F., Bayliss, M. and Doherty, M. (1997) Synovial Fluid Chondroitin and Keratan Sulphate Epitopes, Glycosaminoglycans, and Hyaluronan in Arthritic and Normal Knees. *Annals of the Rheumatic Diseases*, **56**, 299-307. https://doi.org/10.1136/ard.56.5.299

[19] Cameron, M., Buchgraber, A., Passler, H., Vogt, M., Thonar, E., Fu, F., *et al.* (1997) The Natural History of the Anterior Cruciate Ligament-Deficient Knee. Changes in Synovial Fluid Cytokine and Keratan Sulfate Concentrations. *The American Journal of Sports Medicine*, **25**, 751-754.

[20] van den Bosch, M.H.J., van Lent, P.L.E.M. and van der Kraan, P.M. (2020) Identifying Effector Molecules, Cells, and Cytokines of Innate Immunity in OA. *Osteoarthritis and Cartilage*, **28**, 532-543. https://doi.org/10.1016/j.joca.2020.01.016

[21] Bondeson, J., Wainwright, S.D., Lauder, S., Amos, N. and Hughes, C.E. (2006) The Role of Synovial Macrophages and Macrophage-Produced Cytokines in Driving Aggrecanases, Matrix Metalloproteinases, and Other Destructive and Inflammatory Responses in Osteoarthritis. *Arthritis Research & Therapy*, **8**, R187.

[22] Bondeson, J., Blom, A.B., Wainwright, S., Hughes, C., Caterson, B. and van den Berg, W.B. (2010) The Role of Synovial Macrophages and Macrophage-Produced Mediators in Driving Inflammatory and Destructive Responses in Osteoarthritis. *Arthritis & Rheumatism*, **62**, 647-657. https://doi.org/10.1002/art.27290

[23] Farahat, M.N., Yanni, G., Poston, R. and Panayi, G.S. (1993) Cytokine Expression in Synovial Membranes of Patients with Rheumatoid Arthritis and Osteoarthritis. *An-*

nals of the Rheumatic Diseases, **52**, 870-875. https://doi.org/10.1136/ard.52.12.870

[24] Coryell, P.R., Diekman, B.O. and Loeser, R.F. (2021) Mechanisms and Therapeutic Implications of Cellular Senescence in Osteoarthritis. *Nature Reviews Rheumatology*, **17**, 47-57.

[25] Tiulpin, A. and Saarakkala, S. (2020) Automatic Grading of Individual Knee Osteoarthritis Features in Plain Radiographs Using Deep Convolutional Neural Networks. *Diagnostics*, **10**, Article 932.

[26] McKinney, J.M., Pucha, K.A., Bernard, F.C., Brandon, D.J., Doan T.N. and Willett N.J. (2025) Osteoarthritis Early-, Mid- and Late-Stage Progression in the Rat Medial Meniscus Transection Model. *Journal of Orthopaedic Research*, **43**, 102-116.

[27] Huang, N.C., Yang, T.S., Busa, P., Lin, C.L., Fang, Y.C., Chen, I.J. and Wong, C.S. (2021) Detection and Evaluation of Serological Biomarkers to Predict Osteoarthritis in Anterior Cruciate Ligament Transection Combined Medial Meniscectomy Rat Model. *International Journal of Molecular Sciences*, **22**, Article 10179.

[28] Logun, M., Colonna, M.B., Mueller, K.P., Ventarapragada, D., Rodier, R., Tondepu, C., *et al.* (2023) Label-free *in Vitro* Assays Predict the Potency of Anti-Disialoganglioside Chimeric Antigen Receptor T-Cell Products. *Cytotherapy*, **25**, 670-682. https://doi.org/10.1016/j.jcyt.2023.01.008

[29] Kotanchek, M.E., Kotanchek, T. and Kotanchek, K. (2022) Biological Strategies ParetoGP Enables Analysis of Wide and Ill-Conditioned Data from Nonlinear Systems. In: Trujillo, L., Winkler, S.M., Silva, S. and Banzhaf, W., *Genetic Programming Theory and Practice XIX. Genetic and Evolutionary Computation*, Springer, 91-116.

[30] Cheng, A., Vantucci, C.E., Krishnan, L., Ruehle, M.A., Kotanchek, T., Wood, L.B., *et al.* (2021) Early Systemic Immune Biomarkers Predict Bone Regeneration after Trauma. *Proceedings of the National Academy of Sciences*, **118**, e2017889118. https://doi.org/10.1073/pnas.2017889118

[31] Odeh-Couvertier, V., Dwarshuis, N.J., Colonna, M.B., *et al.* (2022) Predicting T-Cell Quality during Manufacturing through an Artificial Intelligence-Based Integrative Multiomics Analytical Platform. *Bioengineering & Translational Medicine*, **7**, e10282.

[32] Palazzo, C., Nguyen, C., Lefevre-Colau, M., Rannou, F. and Poiraudeau, S. (2016) Risk Factors and Burden of Osteoarthritis. *Annals of Physical and Rehabilitation Medicine*, **59**, 134-138. https://doi.org/10.1016/j.rehab.2016.01.006

[33] Watanabe, K., Jose, P.J. and Rankin, S.M. (2002) Eotaxin-2 Generation Is Differentially Regulated by Lipopolysaccharide and IL-4 in Monocytes and Macrophages. *The Journal of Immunology*, **168**, 1911-1918. https://doi.org/10.4049/jimmunol.168.4.1911

[34] Deshmane, S.L., Kremlev, S., Amini, S. and Sawaya, B.E. (2009) Monocyte Chemoattractant Protein-1 (MCP-1): An Overview. *Journal of Interferon & Cytokine Research*, **29**, 313-326. https://doi.org/10.1089/jir.2008.0027

[35] Bickel, M. (1993) The Role of Interleukin-8 in Inflammation and Mechanisms of Regulation. *Journal of Periodontology*, **64**, 456-460.

[36] Hirst, S.J., Hallsworth, M.P., Peng, Q. and Lee, T.H. (2002) Selective Induction of Eotaxin Release by Interleukin-13 or Interleukin-4 in Human Airway Smooth Muscle Cells Is Synergistic with Interleukin-1 β and Is Mediated by the Interleukin-4 Receptor α-Chain. *American Journal of Respiratory and Critical Care Medicine*, **165**, 1161-1171. https://doi.org/10.1164/ajrccm.165.8.2107158

[37] Sonderegger, I., Iezzi, G., Maier, R., Schmitz, N., Kurrer, M. and Kopf, M. (2008) GM-CSF Mediates Autoimmunity by Enhancing Il-6-Dependent Th17 Cell Development

and Survival. *The Journal of Experimental Medicine*, **205**, 2281-2294. https://doi.org/10.1084/jem.20071119

[38] Hirota, K., Hashimoto, M., Ito, Y., Matsuura, M., Ito, H., Tanaka, M., *et al.* (2018) Autoimmune Th17 Cells Induced Synovial Stromal and Innate Lymphoid Cell Secretion of the Cytokine GM-CSF to Initiate and Augment Autoimmune Arthritis. *Immunity*, **48**, 1220-1232.e5. https://doi.org/10.1016/j.immuni.2018.04.009

[39] Molnarfi, N., Benkhoucha, M., Funakoshi, H., Nakamura, T. and Lalive, P.H. (2015) Hepatocyte Growth Factor: A Regulator of Inflammation and Autoimmunity. *Autoimmunity Reviews*, **14**, 293-303. https://doi.org/10.1016/j.autrev.2014.11.013

[40] Litwiniuk, M., Krejner, A., Speyrer, M.S., Gauto, A.R. and Grzela, T. (2016) Hyaluronic Acid in Inflammation and Tissue Regeneration. *Wounds*, **28**, 78-88.

[41] Schneider, R.S., Nieves, E.B., Aggarwal, B., Bowles-Welch, A.C., Stevens, H.Y., Kippner, L.E., *et al.* (2025) On-Chip 3D Potency Assay for Prediction of Clinical Outcomes for Cell Therapy Candidates for Osteoarthritis. *Nature Communications*, **16**, Article No. 4915. https://doi.org/10.1038/s41467-025-60158-w

Supplementary

Table S1. pdSF sample characterization and demographic information used as inputs for SR models.

	Donor info				pdSF sample data								
De-ID Sample No.	KL score	Sex	Age	BMI	Color	SF volume collected (mL)	SF Cell conc. (cells/mL)	Cytokine Profile	Keratan Sulfate conc.	Chondroitin Sulfate conc.	Total protein conc.	Rheology	Electrophoresis grade
1	3	F	54	23.10	Y	Y	Y	Y	Y	Y	Y	Y	--
2	4	M	64	36.41	Y	Y	Y	Y	--	--	Y	--	--
3	3	F	64	32.38	Y	Y	Y	Y	--	--	Y	--	--
4	3	M	58	34.1	Y	Y	Y	Y	--	--	Y	Y	--
5	4	M	63	35.44	Y	Y	Y	Y	Y	Y	Y	Y	Y
6	2	M	62	25.56	Y	Y	Y	Y	Y	Y	Y	Y	Y
7	4	F	64	27.73	Y	Y	Y	Y	--	--	Y	Y	Y
8	4	M	58	32.69	Y	Y	Y	Y	--	--	Y	--	Y
9	3	F	67	25.93	Y	Y	Y	Y	Y	Y	Y	Y	Y
10	4	M	56	34.51	Y	Y	--	Y	--	--	Y	--	--
11	3	F	62	42.93	Y	Y	Y	Y	--	--	Y	Y	Y
12	4	M	60	32.19	Y	Y	--	Y	--	--	Y	--	--
13	3	F	58	27.27	Y	Y	--	Y	--	--	Y	Y	Y
14	2	F	57	21.59	Y	Y	Y	Y	--	--	--	--	--
15	3	F	52	29.65	Y	Y	Y	Y	Y	Y	Y	Y	Y
16	3	F	62	27.22	--	Y	Y	Y	--	--	--	--	--
17	4	M	61	30.11	Y	Y	Y	Y	--	--	Y	--	--
18	2	F	68	24.89	Y	Y	Y	Y	--	--	Y	Y	Y
19	4	M	69	26.52	Y	Y	--	Y	--	--	Y	Y	Y
20	3	M	56	--	Y	Y	Y	Y	--	--	Y	--	--
21	3	M	64	23.68	Y	Y	Y	Y	--	--	Y	--	--
22	4	M	50	26.04	Y	Y	--	Y	--	--	Y	--	--
23	2	M	60	31.71	Y	Y	Y	Y	--	--	--	--	--
24	2	F	62	34.58	Y	Y	Y	Y	--	--	Y	--	Y
25	3	F	58	21.77	Y	Y	Y	Y	--	--	Y	Y	Y
26	4	M	60	38.25	Y	Y	--	Y	--	--	Y	--	Y
27	3	M	58	26.95	--	Y	Y	--	--	--	Y	--	Y
28	3	M	61	24.82	--	Y	--	--	--	--	Y	--	Y
29	3	M	52	32.11	Y	Y	Y	Y	--	--	Y	--	Y
30	3	M	63	28.59	Y	Y	Y	Y	--	--	Y	--	Y
31	2	M	70	29.18	Y	Y	Y	Y	--	--	Y	Y	Y
32	4	M	54	24.63	--	Y	--	--	--	--	Y	--	Y
33	4	F	57	31.8	--	Y	Y	--	--	--	Y	--	Y
34	2	M	67	24.91	Y	Y	Y	Y	--	--	Y	--	Y
35	2	M	51	41.01	Y	Y	Y	Y	--	--	Y	--	Y
36	2	F	59	25.54	Y	Y	Y	Y	--	--	Y	Y	--
37	3	F	60	24.28	Y	Y	Y	Y	--	--	Y	--	--
38	4	F	50	25.83	Y	Y	Y	Y	--	--	Y	--	--
39	4	M	68	23.39	--	Y	Y	--	Y	Y	Y	Y	Y
40	3	M	55	32.69	--	Y	--	Y	--	--	--	Y	Y
41	3	M	67	34.2	--	Y	--	Y	--	--	--	Y	Y

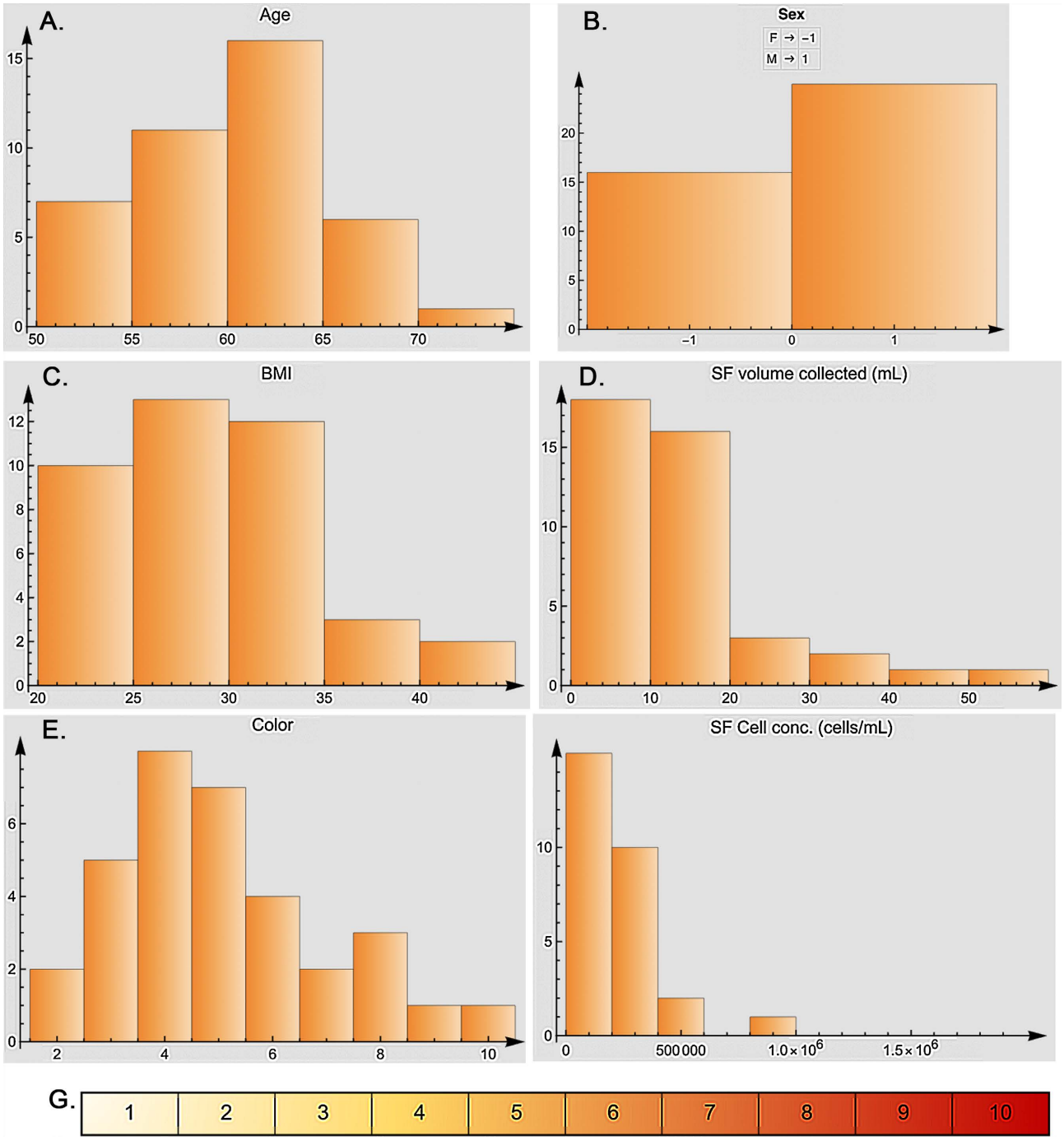

Figure S1. Distribution of data collected at clinical sites related to OA patients (A)-(C) and corresponding pdSF (D)-(F). (G) Color chart used to characterize pdSF color used as an input in SR models.

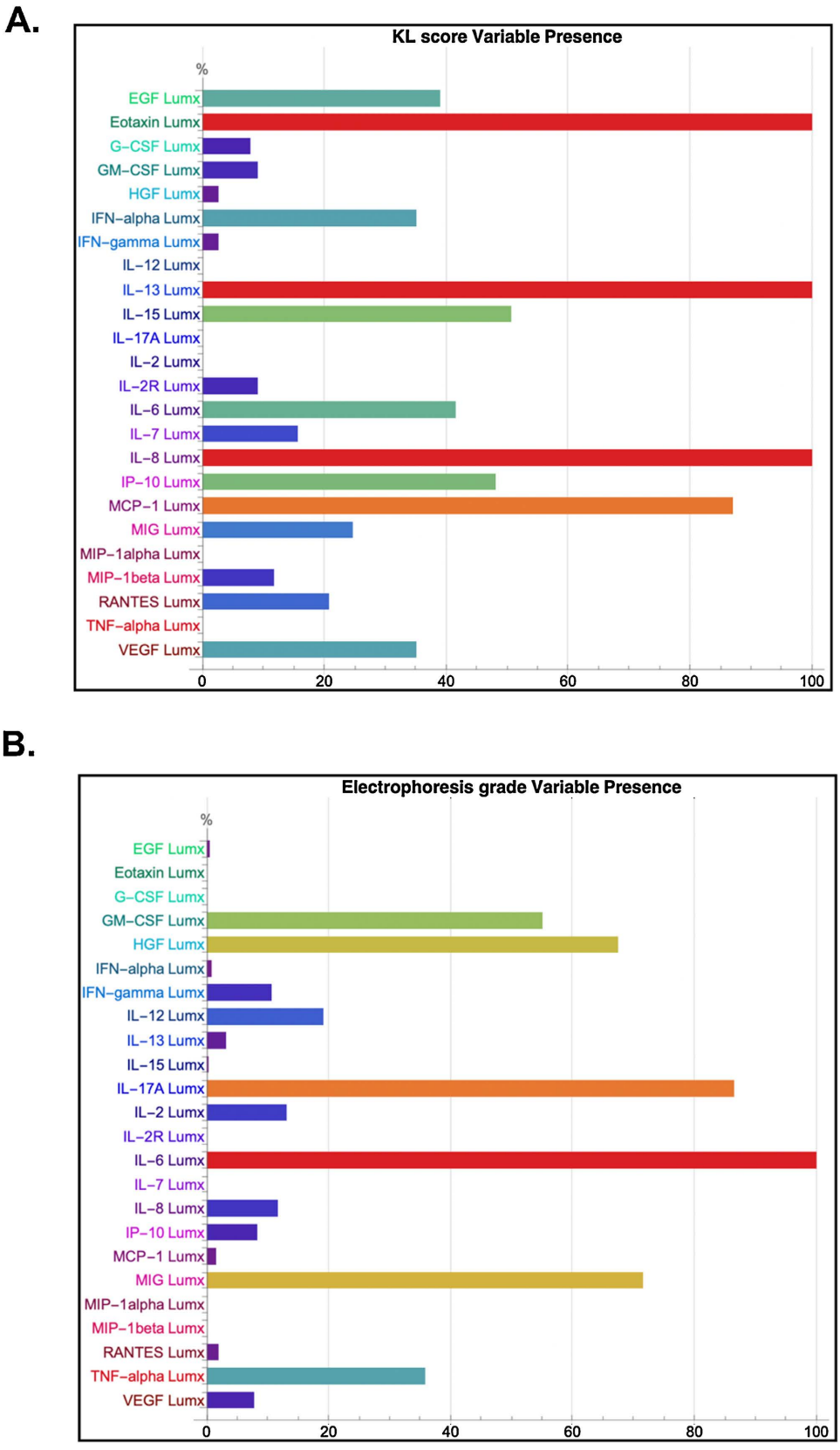

Figure S2. Results of SR models identified top features using only pdSF cytokine data analyzed by Luminex (Lumx). Top features present in all SR models (red) were cytokines correlated to KL score (A) and HA electrophoresis grade (B).

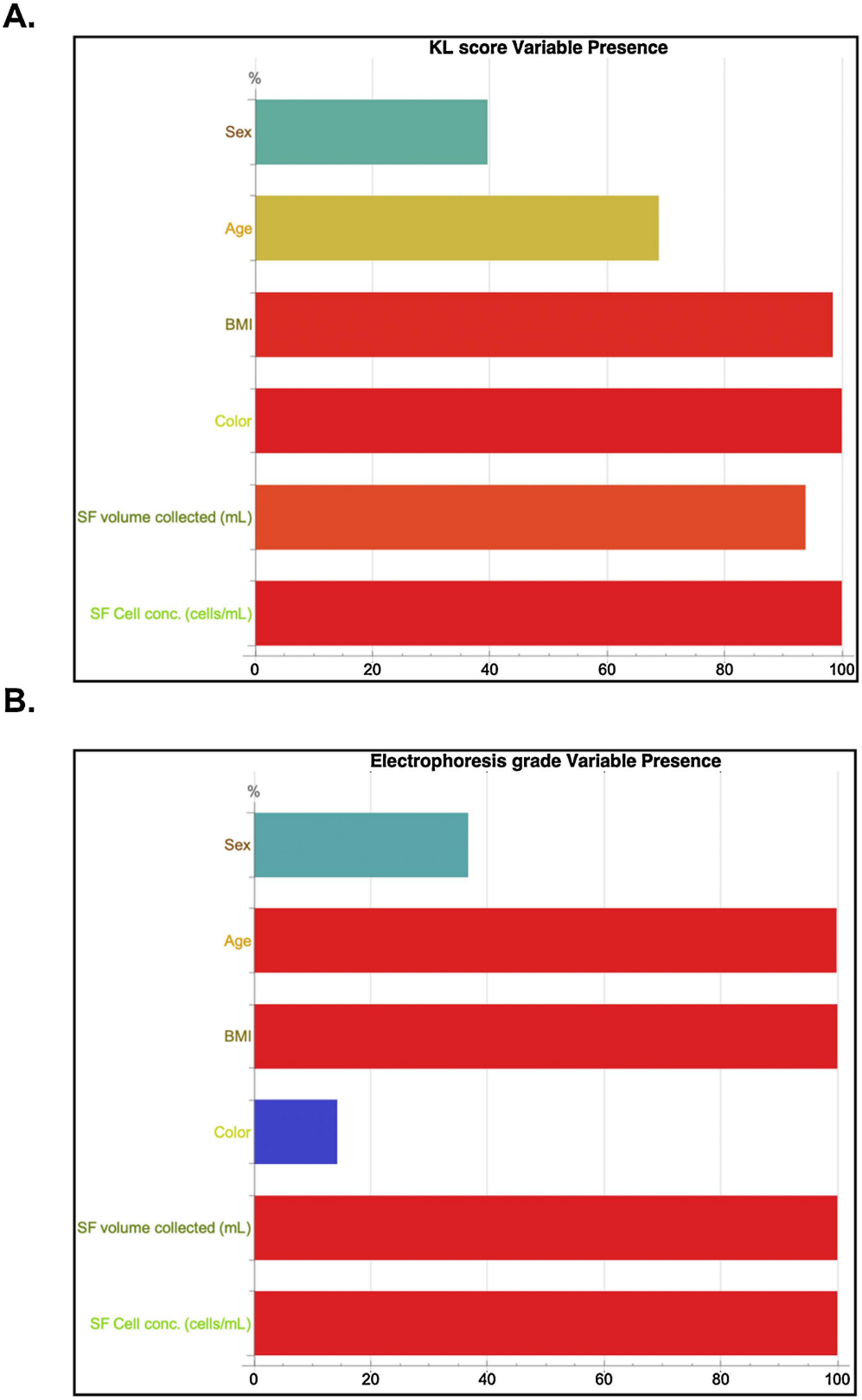

Figure S3. Results of SR models identified top features using only patient demographics and corresponding pdSF information collected at clinical sites. Top features present in the majority of SR models (red) were data correlated to KL score (A) and HA electrophoresis grade (B).